

Liquid Crystalline Poly(propyleneimine) Dendrimers G1–G4: A Chromatographic Study on the Local Ordering of the Terminal Groups

Svetlana V. Blokhina,* Marina V. Ol'khovich, Angelica V. Sharapova, and Nicholas Yu. Borovkov

Institute of Solution Chemistry, Russian Academy of Sciences, 1 Akademicheskaya Street, 153045, Ivanovo, Russia

ABSTRACT: The effect of the generation number on sorption behavior of the liquid crystalline (LC) poly(propyleneimine)dendrimers G1–G4 terminated with *n*-hexadecyl groups has been studied by inverse gas chromatography. To examine the accessibility of the terminal-group shell by small molecules, methyl-substituted derivatives of benzene, pyridine, aniline, and naphthalene have been chosen as probe solutes. The retention volumes and activity coefficients of the solutes are not linearly related to the generation number. The highest thermodynamic solute–solvent compatibility is observed for the dendrimer G2. On the other hand, the highest structural selectivity is observed for the dendrimer G3. The said sorption features are rationalized in terms of local ordering and a higher degree of tightness of the terminal-group shell in the macromolecules of high generations.

INTRODUCTION

Dendrimers are structurally perfect cascade polymers with a regular and highly branched molecular architecture.¹ Their monodisperse nature, molecular dimensions, and globular shape make them a promising platform for the creation of functional core–shell structures.² The easy control of these features offers ideas to apply dendrimers as nanocatalysts, drug-delivery agents, optical materials, and so forth.

Data on interaction of dendrimers with volatile substances are of use in the design of chemical sensors, filters, membranes, sorbents, and chromatographic materials.³ Dendritic macromolecules with mesogenic terminal groups behave as liquid crystalline (LC) materials.⁴ Dendrimers are generally disordered entities;⁵ therefore, the LC ordering may offer new scientific and applied opportunities.

Liquid crystals of low molar mass are being applied in analytical chromatography for a long time as highly selective sorbents of isomeric aromatic substances. Their structural selectivity was first revealed about half a century ago^{6,7} and recently reviewed in ref 8. Moreover, the gas chromatography technique was found to be a useful tool to determine thermodynamic characteristics of dissolution of organic substances in the LC phases of rod-like mesogens of low molar mass⁹ and linear polymers.¹⁰ Nonetheless, thermodynamic studies on LC polymers with a branched molecular structure seem scarce so far.¹¹ Liquid chromatography was applied¹² to demonstrate selective sorption of polycyclic hydrocarbons with various molecular geometry peculiarities by laterally substituted LC polymers. A mechanistic interpretation of geometric recognition of solutes through steric effects of the alkyl-groups of brush-like branched polymers was developed.¹³ Activity coefficients of polar and nonpolar solutes were obtained at infinite dilution in the amorphous phase of the polymeric amine¹⁴ and carbosilane¹⁵ species. One of these studies¹⁴ revealed the relationship between the activity coefficients and generation number of the polyamidoamine dendrimers to be nonlinear.

Two features of the LC dendrimers seem of special note: first, a large free volume determined by the molecular core, and second, a multitude of loosely packed terminal groups where the amount

increases in geometric progression with the generation number.¹⁶ The latter feature enables programming the molecular functionality and fine-tuning the interactions with molecular objects and surfaces.¹⁷ Recently we used the inverse gas chromatography (IGC) technique to study a number of systems based on the *n*-hexadecyl-terminated LC poly(propyleneimine)dendrimers (Figure 1). The structural selectivity of the dendrimers for isomeric xylenes was revealed in ref 18. In our next work,¹⁹ the mesomorphous behavior of the pure dendrimers was studied. The first-order nature of all phase transitions from the mesophase to isotropic liquid state was stated. Subsequently the effect of the generation number on sorption of *n*-alkanes and *n*-alcohols was investigated.²⁰ The recent work²¹ deals with the thermodynamics of dissolution of *n*-alkanes and *n*-alcohols in the binary LC system composed of the dendrimer G2 and the nematic derivative of cyanobiphenyl. In particular, solute–solvent compatibility was characterized by the activity coefficients and revealed to be dependent nonlinearly on the composition of the LC sorbent.

Further steps in this direction seem reasonable in the light of the works^{22,23} where the vapor–liquid equilibria were studied by static measurements on dendrimers with various terminal groups and generation numbers. Researchers^{22,23} found no regular features in sorption behavior of the dendrimers and concluded the measurements to be most informative in the field of low solute concentrations. In connection with important application aspects,⁴ through personal^{18–21} and outsider^{22,23} experiences, this work has been planned to reveal the interplay among the generation number, phase state, and spatial ordering of the peripheral groups in *n*-hexadecyl-terminated dendritic macromolecules.

EXPERIMENTAL SECTION

Materials. The 3,4-di(hexadecyloxybenzoyl)poly(propyleneimine) dendrimers G1–G4 were synthesized in the University of

Received: July 15, 2011

Accepted: September 27, 2011

Published: October 19, 2011

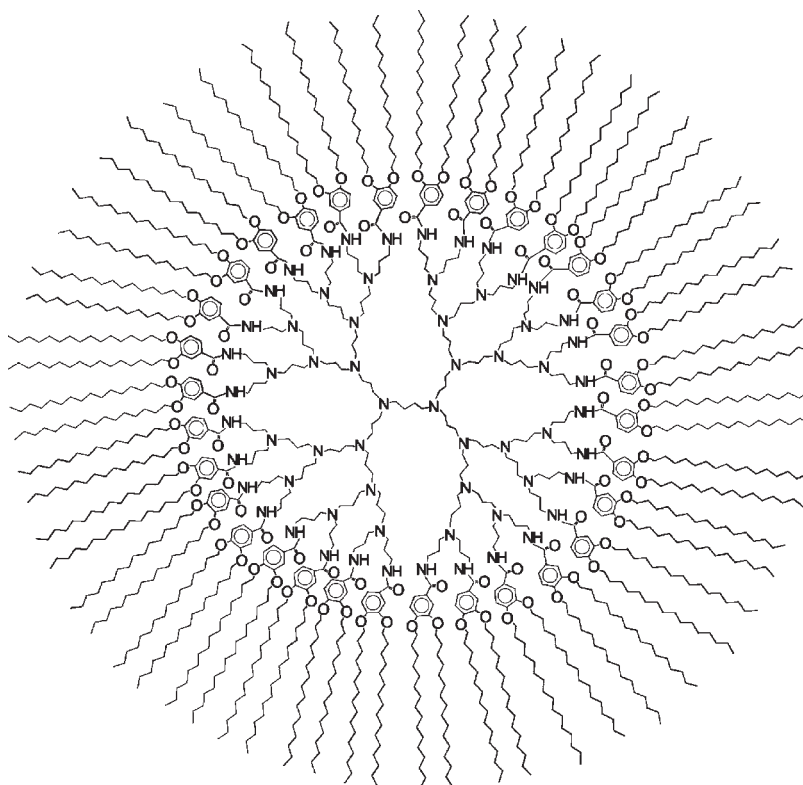


Figure 1. Molecular structure of the dendrimer G4.

Table 1. Phase Transition Temperatures for the Dendrimers G1–G4

dendrimer no.	molecular mass	terminal group no.	phase transitions ^a (K)
G1	3095	4	Cr 335 Col ₁ 375 Col ₂ 385 Is
G2	5439	8	Cr 331 Col 387 Is
G3	10302	16	Cr 329 Col 386 Is
G4	22182	32	Cr 384 Is

^a Abbreviations: Cr, crystalline (glassy) phase; Col, hexagonal columnar mesophase; Is, isotropic phase.

Bayreuth (Germany) and kindly presented for chromatographic studies by Prof. G. Latterman. Structural identification was conducted by the elemental analysis, thermogravimetry, and IR, ¹H NMR, mass, and electron spectroscopy techniques. The purity of the dendrimers determined by size exclusion chromatography was 98 %. The corresponding preparative procedure was described in ref 24. The molecular structure of the dendrimer G4 is shown in Figure 1. Phase transition temperatures (Table 1) were acquired by polarizing microscopy and differential scanning calorimetry (DSC) on preliminarily vitrified samples.

Benzene, pyridine, *p*-, *m*-, and *o*-xylenes, 3,4- and 3,5-lutidines, *p*- and *m*-toluidines, and α - and β -methylnaphthalenes (all of 99 % purity from Aldrich, St. Louis, MO, USA) were used as volatile probe solutes.

Apparatus and Procedure. The sorption behavior of the dendrimers was studied on a gas chromatograph “Chrom-5” (Laboratory Instruments Works, Prague, Czech Republic) equipped

with a flame-ionization detector operating in the isothermal mode. The temperature was kept within ± 0.1 K. The dendrimers were deposited onto a solid support, namely, Chromaton N AW-DMCS, (0.125 to 0.160) mm (Chemapol, Prague, Czech Republic), from solutions in tetrahydrofuran. In all cases the 10 ± 0.2 % mass loading was used. The dendrimer content in the sorbent was determined from a mass loss upon annealing in an oven of a 1000B MOM derivatograph (Hungary). Glass microcolumns (0.4 m \times 1 mm) were packed in vacuum. Before every experimental series, the columns were heated to 403 K, cooled down to the room temperature, and then heated again to a desired point. The temperature was kept constant within ± 0.2 K by the air bath. The chromatographic columns were placed in the middle of the bath, where the temperature gradient along the column was checked to be within ± 0.5 K.

The gas carrier was 99.99 % helium. The flow rate was 25 ± 0.1 mL \cdot min⁻¹ by a bubble flow meter. A membrane manometer with precision of 0.1 bar was used to measure the column-inlet pressure. The column-outlet pressure being equal to the atmospheric one was measured by a barometer with precision of 1 mbar. A 1 μ L microsyringe (Hamilton, Switzerland) was used for injection. To measure the void time, methane was used. In every experimental run, at least five measurements were performed to ensure a good reproducibility of the data; deviations from the average value fell within ± 0.5 %. Experimental errors were estimated using the Student coefficients with the confidence probability of 0.95. The relative error for V_g^0 is 3 %. A contribution of adsorption on the solid support into retention was annihilated by silanization. In addition, no dependence of the retention volume on the stationary phase loading was observed, indicating that surface sorption effects are insignificant compared with bulk sorption.

BACKGROUND

Thermodynamically important sorption characteristics can be found from IGC data, namely, retention time, t_R , and specific retention volumes, V_g^0 , of volatile solutes:²⁵

$$V_g^0 = (t_R - t_M)F_{p,T}j_2^3 \left(\frac{273}{T} \right) / W_L \quad (1)$$

Above, t_R and t_M are the retention time of a solute and “unretained” component (methane), respectively; $F_{p,T}$ is the flow rate of the gas carrier measured at a column outlet at column temperature $T = 273.16$ K and pressure $p = 760$ mm, W_L is the mass of the LC sorbent in a column, and j_2^3 is the James–Martin coefficient²⁵

$$j_2^3 = \frac{3(p_i/p_o)^2 - 1}{2(p_i/p_o)^3 - 1} \quad (2)$$

where p_i and p_o are the inlet and outlet pressures.

The mass fraction activity coefficient at infinite dilution, $(a_1/w_1)^\infty$, is calculated from the equation:²⁶

$$\ln(a_1/w_1)^\infty = \ln \frac{273.2R}{V_g^0 p_1^0 M_1} - \frac{p_1^0}{RT} (B_{11} - V_1) \quad (3)$$

Above, a_1 and w_1 are the activity and mass fraction of a solute; p_1^0 is the pressure of saturated vapor of a solute at T ; B_{11} and V_1 are the second virial coefficient and molar volume of a solute; M_1 is the molar mass of a solute.

The mass fraction activity coefficient is connected with the partial molar free energy of mixing, ΔG_1^∞ , by the ratio:

$$\Delta G_1^\infty = RT \ln(a_1/w_1)^\infty = \Delta H_1^\infty - T\Delta S_1^\infty \quad (4)$$

The partial molar enthalpy, ΔH_1^∞ , and entropy, ΔS_1^∞ , of mixing of a solute were assumed to be temperature-independent and found from the $\ln(a_1/w_1)^\infty - (1/T)$ relationship.

The partial molar enthalpies and entropies of solute dissolution, ΔH_s and ΔS_s , are calculated from the equations:

$$\Delta H_s = -R \frac{\partial \ln V_g^0}{\partial (1/T)} \quad (5)$$

$$\Delta S_s = \Delta S_1^\infty - (\Delta H_1^\infty - \Delta H_s)/T \quad (6)$$

Above, R is the universal gas constant.

In general, the dissolution of a solute vapor in a liquid sorbent can be represented as a sequence of two stages: condensation of the vapor resulting in the liquid-phase solute and dissolution of the liquid-phase solute in the liquid sorbent resulting in the infinitely diluted solution. The vaporization enthalpies for pure solutes, ΔH_v , may be calculated from the ΔH_1^∞ and ΔH_s values:

$$\Delta H_v = \Delta H_1^\infty - \Delta H_s \quad (7)$$

The IGC technique is appropriate provided that a whole bulk of a LC sorbent participates in the distribution of a volatile solute; as a result, the local solvent–solute equilibrium is expected to be established. Our experiment has shown that diffusion-imposed restrictions of the IGC approach do not impede chromatographic studies on the LC dendrimers because of the large gas permeability of the dendritic materials.

The fact that the measurements were done at equilibrium in the region of Henry's law is evidenced by the independence of the retention time of each solute from the volume of an injected

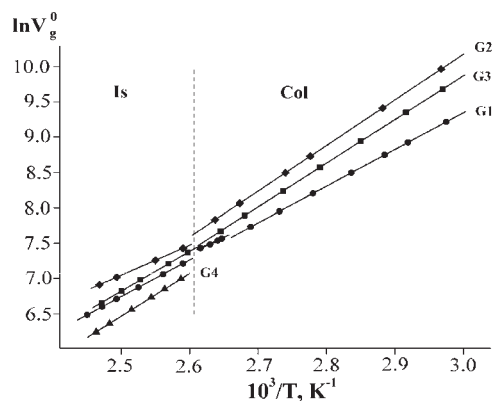


Figure 2. Retention diagram of *p*-toluidine in the columnar (Col) and isotropic (Is) phases of the dendrimers G1–G4.

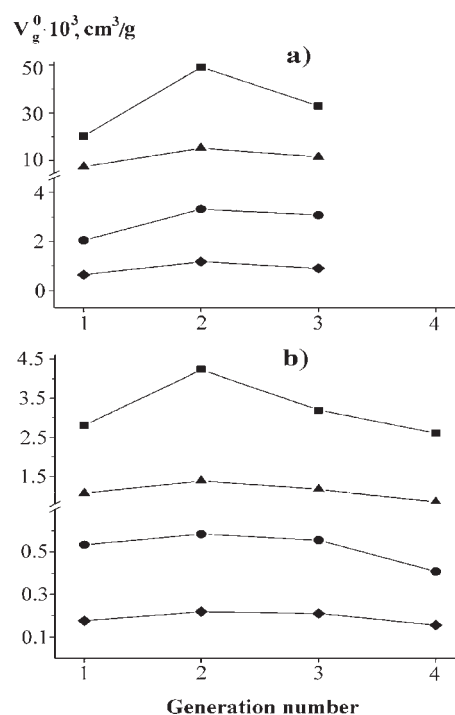


Figure 3. Specific retention volume of the solutes versus the generation number in the columnar (a) and isotropic (b) phases of the dendrimers G1–G4: \blacklozenge , *o*-xylene; \bullet , 3,4-lutidine; \blacktriangle , *m*-toluidine; \blacksquare , α -methylnaphthalene.

solute, the high symmetry of the chromatographic peaks, and the linear relation for each solute between the logarithm of the specific retention volume and reciprocal temperature.

The separation factor for the structural isomers has been calculated from the equation:

$$\alpha_{1/2} = V_{g_2}^0 / V_{g_1}^0 \quad (8)$$

Here the indexes 1 and 2 correspond to the elution sequence. The differences in the thermodynamic characteristics of isomer dissolution, $\Delta(\Delta H)_{2/1}$ and $\Delta(\Delta S_s)_{2/1}$, were calculated from the temperature dependence of the logarithmic separation factor according to the equation:²⁷

Table 2. Thermodynamic Characteristics for the Solutes in the Columnar Phases of the Dendrimers G1–G3 at Infinite Dilution and $T = 343 \text{ K}^a$

solute	$(a_1/w_1)^\infty$	ΔH_s	ΔS_s	ΔH_1^∞	ΔS_1^∞	ΔH_v	ΔH_v^a	
		$\text{kJ}\cdot\text{mol}^{-1}$	$\text{J}\cdot\text{mol}^{-1}\cdot\text{K}^{-1}$	$\text{kJ}\cdot\text{mol}^{-1}$	$\text{J}\cdot\text{mol}^{-1}\cdot\text{K}^{-1}$	$\text{kJ}\cdot\text{mol}^{-1}$	$\text{kJ}\cdot\text{mol}^{-1}$	
G1	<i>m</i> -xylene	4.03	-25.0	-84.6	15.0	32.1	40.0	40.7
	<i>p</i> -xylene	3.82	-25.4	-85.1	14.3	30.6	39.7	40.2
	<i>o</i> -xylene	4.01	-26.2	-88.0	14.5	30.8	40.7	41.3
	3,4-lutidine	4.10	-27.5	-91.8	17.6	39.8	45.1	
	3,5-lutidine	4.31	-27.0	-90.8	17.8	39.7	44.8	
	<i>p</i> -toluidine	4.39	-41.9	-134.6	11.1	20.1	53.0	54.6
	<i>m</i> -toluidine	4.22	-43.2	-138.0	10.7	19.3	54.0	54.3
	α -methyl-naphthalene	4.31	-46.6	-148.0	10.7	19.2	57.4	56.2
	β -methyl-naphthalene	3.94	-50.2	-157.7	6.1	6.3	56.2	56.3
G2	<i>m</i> -xylene	2.28	-36.5	-113.2	3.2	2.6	39.73	40.7
	<i>p</i> -xylene	2.01	-36.7	-113.4	2.9	2.0	39.44	40.2
	<i>o</i> -xylene	2.23	-38.0	-117.4	2.7	1.2	40.52	41.3
	3,4-lutidine	2.59	-41.1	-127.7	4.1	4.1	45.20	
	3,5-lutidine	2.61	-40.3	-125.5	3.9	3.4	44.23	
	<i>p</i> -toluidine	2.16	-52.0	-158.0	-0.1	-6.8	51.88	54.6
	<i>m</i> -toluidine	1.99	-53.7	-162.4	-0.9	-8.5	52.78	54.3
	α -methyl-naphthalene	1.75	-58.7	-175.9	-2.5	-11.9	56.21	56.2
	β -methyl-naphthalene	1.68	-60.4	-180.5	-5.1	-19.1	55.35	56.3
G3	<i>m</i> -xylene	2.97	-33.2	-106.0	6.7	10.4	39.91	40.7
	<i>p</i> -xylene	2.75	-33.6	-106.6	5.9	8.9	39.61	40.2
	<i>o</i> -xylene	2.80	-34.3	-108.7	6.3	9.7	40.63	41.3
	3,4-lutidine	1.07	-37.3	-117.8	8.0	14.3	45.24	
	3,5-lutidine	1.11	-36.1	-114.5	8.4	15.2	44.5	
	<i>p</i> -toluidine	3.13	-48.3	-147.3	3.8	4.6	52.09	54.6
	<i>m</i> -toluidine	2.72	-51.5	-158.5	2.2	-1.9	53.71	54.3
	α -methyl-naphthalene	2.69	-53.5	-164.3	3.9	3.0	57.4	56.2
	β -methyl-naphthalene	2.75	-54.7	-168.0	1.7	-3.4	56.45	56.3

^a Notes: The relative errors at 95 % confidence are: 3.1 % for $(a_1/w_1)^\infty$; 3.2 % for ΔH_1^∞ and ΔH_s ; 3.6 % for ΔS_1^∞ and ΔS_s ; 4 % for ΔH_v .

$$\ln \alpha_{1/2} = \frac{-(\Delta H_s)_1 + (\Delta H_s)_2}{RT} + \frac{(\Delta S_s)_1 - (\Delta S_s)_2}{R}$$

$$= \frac{\Delta(\Delta H_s)_{2/1}}{RT} - \frac{\Delta(\Delta S_s)_{2/1}}{R} \quad (9)$$

The retention indexes were calculated from the equation:²⁸

$$I = 100 \frac{\log t'_{Rz} - \log t'_{R(z+1)}}{\log t'_{Rz} - \log t'_{Rz}} + 100z \quad (10)$$

Here the z symbol is a number of carbon atoms in a normal alkane that exits the column before the probe solute under consideration; the $(z + 1)$ symbol is a number of carbon atoms in a normal alkane that exits the column immediately after the probe solute.

RESULTS AND DISCUSSION

The dendrimers G1–G4 have been chosen for two reasons. First, their molecules have brush-like alkyl-groups which are known to determine sorption behavior of hyper-branched polymers.¹² Second, their LC phases exist within the closely overlapping temperature ranges and, thus, may be directly compared thermodynamically. The chromatographic data have been used

to determine temperature dependence of the specific retention volume V_g^0 for the said solutes at temperatures ranging from (333 to 408) K. As an example, Figure 2 shows the $\ln V_g^0 - 1/T$ plots for *p*-toluidine. All plots clearly exhibit a common feature: their slope suffers abrupt changes at the phase transition temperature. This indicates that the local structure of the sorbent, in which the solute molecules are incorporated, suffers changes upon the phase transitions. For all solutes, these changes are less pronounced in the case of the dendrimer G3. This fact seems to be connected with the low phase-transition enthalpy for this dendrimer.¹⁹ Corresponding temperatures determined from these plots are in good agreement with the data¹⁹ acquired by DSC and polarizing light microscopy (Table 1).

As a first step, the dependencies of the V_g^0 volume of the solutes on the generation number have been studied (Figure 3). The highest sorption capacity and hence a free volume available for the solute molecules are observed for the dendrimer G2. The dendrimer G3 having a larger core volume exhibits a bit lower V_g^0 values. Such a feature is observed both in the columnar and isotropic phases. The dendrimer G4 does not form the LC phase, but the V_g^T values for its isotropic phase are lower than ones for the dendrimer G3 and, thus, indicate the decreasing retention with increasing the number. One should note that this feature was not revealed in the case of normal alkanes and alcohols.²⁰ Thus, the

Table 3. Thermodynamic Characteristics for the Solutes in the Isotropic Phases of the Dendrimers G1–G4 at Infinite Dilution and $T = 387\text{ K}^a$

	solute	$(a_1/w_1)^\infty$	ΔH_s	ΔS_s	ΔH_1^∞	ΔS_1^∞	ΔH_v	ΔH_v^a
			$\text{kJ}\cdot\text{mol}^{-1}$	$\text{J}\cdot\text{mol}^{-1}\cdot\text{K}^{-1}$	$\text{kJ}\cdot\text{mol}^{-1}$	$\text{J}\cdot\text{mol}^{-1}\text{K}^{-1}$	$\text{kJ}\cdot\text{mol}^{-1}$	$\text{kJ}\cdot\text{mol}^{-1}$
G1	<i>m</i> -xylene	2.41	−37.3	−101.9	1.3	−3.8	38.5	37.2
	<i>p</i> -xylene	2.29	−34.5	−94.6	1.6	−2.8	36.1	37.7
	<i>o</i> -xylene	2.34	−36.2	−99.3	3.1	0.5	39.2	38.4
	3,4-lutidine	2.13	−30.9	−85.0	14.1	29.6	45.0	
	3,5-lutidine	2.26	−29.3	−81.4	13.2	26.9	42.5	
	<i>p</i> -toluidine	2.66	−41.9	−114.8	9.0	14.8	50.9	51.2
	<i>m</i> -toluidine	2.46	−43.2	−117.4	6.9	10.1	50.1	51.3
	α -methylnaphthalene	2.51	−53.5	−143.7	0.7	−5.9	54.1	53.6
	β -methylnaphthalene	2.64	−52.0	−140.4	1.4	−4.4	53.4	53.7
G2	<i>m</i> -xylene	1.95	−37.4	−100.7	1.2	−2.5	38.6	37.2
	<i>p</i> -xylene	1.90	−37.3	−100.4	0.9	−3.0	38.2	37.7
	<i>o</i> -xylene	1.93	−37.1	−100.0	2.1	−0.1	39.2	38.4
	3,4-lutidine	2.01	−41.4	−111.1	3.9	4.2	45.3	
	3,5-lutidine	2.14	−39.6	−104.4	2.8	0.9	42.4	
	<i>p</i> -toluidine	2.18	−30.8	−84.8	19.3	42.5	50.1	51.2
	<i>m</i> -toluidine	2.16	−35.2	−96.0	18.0	39.4	53.2	51.3
	α -methylnaphthalene	1.68	−53.6	−140.8	1.1	−1.7	54.7	53.6
	β -methylnaphthalene	1.75	−52.8	−139.0	0.4	−3.7	53.2	53.7
G3	<i>m</i> -xylene	2.07	−28.0	−77.3	10.2	20.0	38.2	37.2
	<i>p</i> -xylene	1.97	−28.6	−78.5	9.3	18.0	37.9	37.7
	<i>o</i> -xylene	1.99	−27.9	−76.9	10.9	21.9	38.8	38.4
	3,4-lutidine	2.18	−39.1	−106.1	5.2	6.8	44.3	
	3,5-lutidine	2.20	−38.2	−103.8	5.0	6.3	43.2	
	<i>p</i> -toluidine	0.98	−45.5	−123.9	4.8	4.0	50.3	51.2
	<i>m</i> -toluidine	0.91	−46.8	−126.8	4.3	3.3	51.2	51.3
	α -methylnaphthalene	2.20	−52.8	−140.8	1.5	−2.8	54.3	53.6
	β -methylnaphthalene	2.46	−50.0	−134.9	3.4	1.2	53.4	53.7
4	<i>m</i> -xylene	2.69	−30.2	−85.0	7.1	9.8	37.3	37.2
	<i>p</i> -xylene	2.53	−30.9	−86.5	7.2	10.5	38.1	37.7
	<i>o</i> -xylene	2.66	−32.0	−89.6	9.5	16.1	41.5	38.4
	3,4-lutidine	2.97	−21.9	−64.7	22.5	48.3	44.4	
	3,5-lutidine	3.19	−20.8	−62.5	22.1	46.7	42.9	
	<i>p</i> -toluidine	3.53	−46.0	−127.5	2.5	−4.4	48.5	51.2
	<i>m</i> -toluidine	3.49	−50.3	−138.5	1.9	−5.5	52.2	51.3
	α -methylnaphthalene	2.69	−50.9	−137.8	3.5	0.8	54.2	53.6
	β -methylnaphthalene	2.80	−46.4	−126.6	7.3	10.1	53.7	53.7

^a Notes: The relative errors are as in Table 2.

molecular structure of the dendrimers restricts only the sorption of aromatic solutes, whereas the sterically flexible alkanes fit themselves into the brush-like shell.

The thermodynamic characteristics (Tables 2 and 3) have been calculated from the temperature dependencies of the V_g^0 quantities. The reliability thereof is evidenced by good agreement of all experimental enthalpies of solute evaporation, ΔH_v , with the enthalpies calculated by the Watson relation, ΔH_v^* .²⁹

Figure 4 shows the typical $\ln(a_1/w_1)^\infty - 1/T$ plots for *o*- and *p*-xylenes. All plots are linear for both columnar and isotropic phases, the correlation factor being not less than 0.996. The activity coefficients depend on temperature inversely. In the case of the columnar phase, the $(a_1/w_1)^\infty$ values exceed the unity and, thus, indicate the positive deviation of the binary systems from

ideality. Such a feature is typical for classic mesomorphous solvents.⁹

Relationships between the activity coefficients and generation number are given in Figure 5. They indicate that the lowest $(a_1/w_1)^\infty$ values and hence highest thermodynamic compatibility of the solutes with both liquid phases are observed for the dendrimer G2. The higher activity coefficients for the dendrimer G3 and especially G4 (Figure 5b) indicate a trend of decreasing compatibility with increasing the generation number. Only the first member of the row G1–G4 does not follow this trend. The minimum on the $\ln(a_1/w_1)^\infty - 1/T$ plots was revealed also for amino-terminated dendrimers.¹⁴ Thus, the dendrimers of the medium generations exhibit thermodynamic peculiarities of scientific interest.

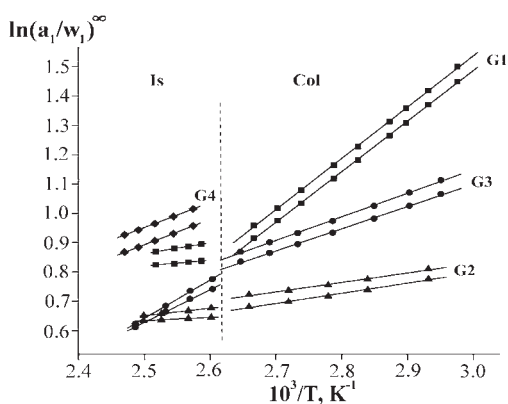


Figure 4. Logarithm of the weight-fraction activity coefficient of *o*- and *p*-xylenes versus reciprocal temperature in the columnar and isotropic phases of the dendrimers G1–G4.

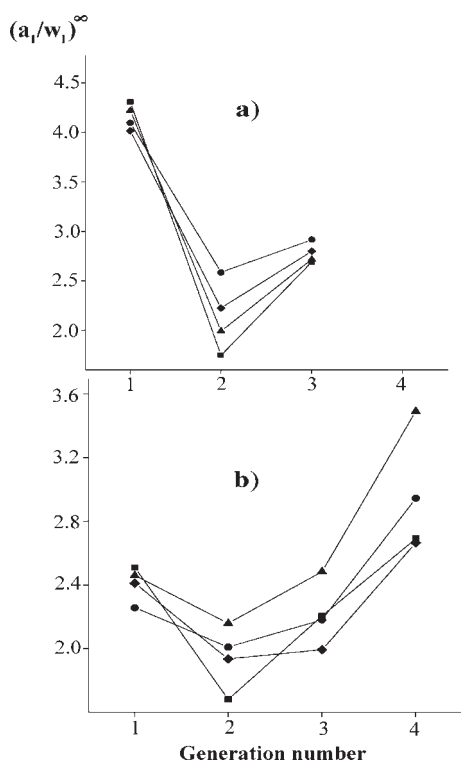


Figure 5. Weight-fraction activity coefficient of the solutes versus the generation number in the columnar (a) and isotropic (b) phases of the dendrimers G1–G4: \blacklozenge , *o*-xylene; \bullet , 3,4-lutidine; \blacktriangle , *m*-toluidine; and \blacksquare , α -methyl-naphthalene.

For the hydrocarbon solutes, that is, xylenes and methyl-naphthalenes, the differences between the partial molar enthalpies (ΔH_s in Table 2) for the isomers may be attributed to geometrical anisotropy favoring the alignment of the solute molecules with the terminal alkyl groups. The alignment is expected to be more efficient for *p*-xylene and β -methyl-naphthalene than for *m*-xylene and α -methyl-naphthalene, respectively. Under the circumstances, the contribution of dispersion solute–solvent attraction is higher for the former solutes. In the case of the isotropic phase (Table 3), the differences between the ΔH_s values for isomeric xylenes and naphthalenes indicate the preservation of the

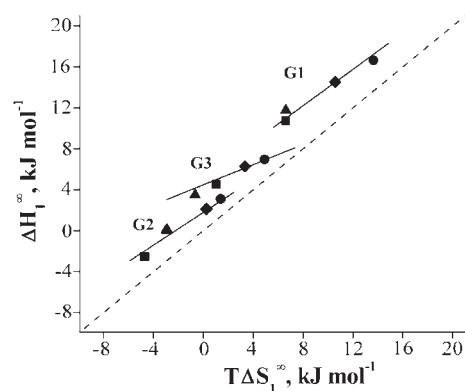


Figure 6. Correlations of the enthalpy and entropy contributions into the Gibbs energy in the columnar phase of the dendrimers G1–G3: \blacklozenge , *o*-xylene; \bullet , 3,4-lutidine; \blacktriangle , *m*-toluidine; \blacksquare , α -methyl-naphthalene. The dashed line is a bisector corresponding to the quasi-ideal solutions with the unity activity coefficient.

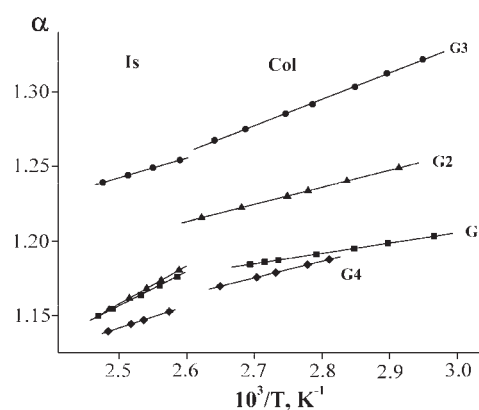


Figure 7. Separation factor for 3,4-/3,5-lutidines versus reciprocal temperature in the columnar and isotropic phases of the dendrimers G1–G4.

said alignment in the isotropic phase. The higher negative ΔH_s and ΔS_s values for methyl naphthalenes as compared with ones for xylenes may be safely attributed to the higher polarizability of the two-ring molecules. As for the nitrogenous solutes, the ΔH_s values for isomeric xylenes and lutidines are close enough to suppose a lack of the dipole interaction. Consequently, in the case of strongly retained toluidines, the polarizability factor rather than dipole-driven attraction prevails as well. Thus, the penetration of the solute molecules into the core is hardly possible under the experimental conditions, and hence, thermodynamic dendrimer–solute compatibility is most probably governed by the free volume confined within a shell of the terminal alkyl groups. In the case of the dendrimers G2–G4, the supramolecular structure of the shell is expected to compactify gradually with the generation number increasing.¹⁶ As for the lowest analogue G1, the voids located between its radially diverging alkyl groups may favor intermolecular overlapping. As a consequence, the packing density increases, and dissolving becomes hampered.

Figure 6 compares the enthalpy and entropy contributions into the Gibbs energy of dissolution, ΔH_1^∞ and ΔS_1^∞ , respectively. The experimental points located above the bisector indicate that the enthalpy contribution prevails in all cases. Hence the positive deviation of the solute–solvent systems from ideality is

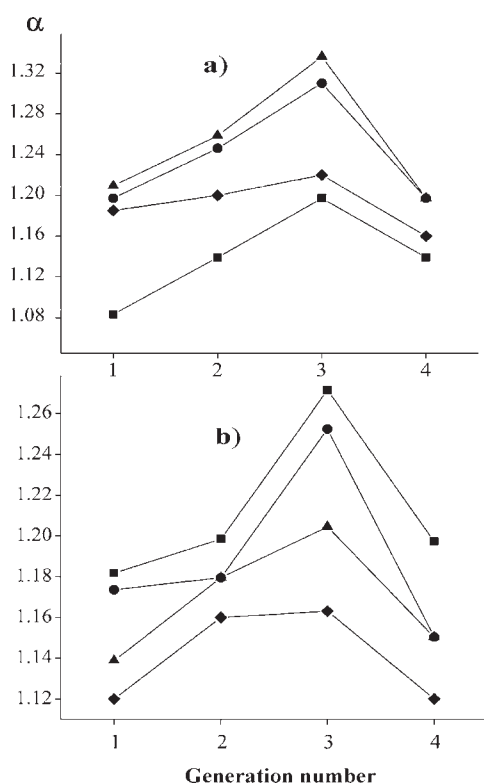


Figure 8. Separation factor versus the generation number of the dendrimers G1–G4 in the columnar phase at 343 K (a) and in the isotropic phase at 387 K (b): \blacklozenge , *o*-/*p*-xylene; \bullet , 3,4-/3,5-lutidine; \blacktriangle , *m*-/*p*-toluidine; \blacksquare , α -/ β -methylnaphthalene. Note: the data on the dendrimer G4 at 343 K refer to the glassy phase.

Table 4. Retention Indexes for the Structure-Sensitive Solutes and Corresponding Methyl Group Increments^a

solute	G1		G2		G3		G4	
	<i>I</i>	ΔI	<i>I</i>	ΔI	<i>I</i>	ΔI	<i>I</i>	ΔI
<i>m</i> -xylene	927	107	951	130	975	136	906	98
<i>p</i> -xylene	929	108	955	132	981	139	911	101
<i>o</i> -xylene	953	120	977	143	1007	152	926	108
3,5-lutidine	1102	132	1104	149	1141	150	1140	144
3,4-lutidine	1124	143	1132	163	1187	173	1178	163

^a Notes: (1) The probe solutes are given in accordance with their boiling points. (2) The increments for xylenes and lutidines were calculated by the equation $\Delta I = (I - I_0)/2$, where I_0 stands for the index of the reference probes, benzene, and pyridine, respectively. (3) All values refer to 373 K, that is, to the columnar phase of the dendrimers G1–G3 and the glassy state of the dendrimer G4.

determined by the heat effects of mixing of the solutes with the liquid dendrimers. The lowest positive and even negative ΔH_1^∞ and ΔS_1^∞ values are observed in the case of the dendrimers G2 and G3. In the case of the analogue G1, the high endoeffects accompanied by the fairly high entropy changes are observed. Thus, the solutes exhibit relatively high compatibility with the dendrimers G2 and G3, whereas the access thereof into the structure of the analog G1 is noticeably hampered.

As stated above, the nonlinear dependence of the solute–solvent interaction on the generation number seems to be connected

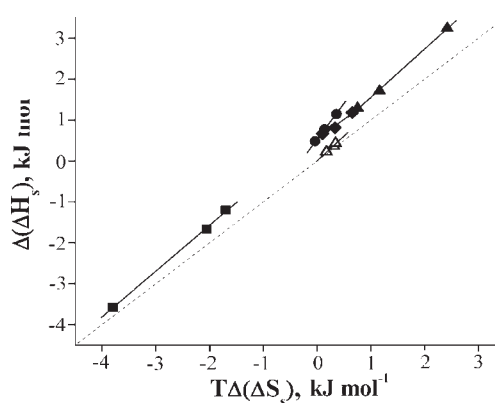


Figure 9. Correlations of the enthalpy and entropy contributions into the separation factor in the columnar phase (343 K) of the dendrimers G1–G3: \triangle , *p*-/*m*-xylenes; \blacklozenge , *o*-/*p*-xylenes; \bullet , 3,4-/3,5-lutidines; \blacktriangle , *p*-/*m*-toluidines and \blacksquare , α -/ β -methylnaphthalenes. The dashed line is a bisector.

with packing features of the terminal alkyl groups. Therefore, the sorption of isomeric hydrocarbons and amines has been studied for further understanding the dissolution mechanism. The retention data indicate that the isomers are typically eluted in accordance with their boiling temperatures. Thus, separation is determined by the saturated vapor pressure factor. The elution order is inverted only for *p*- and *m*-xylenes, being a well-known test couple for revealing the structural selectivity of sorbents. Relatively more efficient dissolution of *p*-xylene is obviously connected with the intermolecular alignment resulting in strengthening of the dispersion solute–solvent interactions.

In all cases, the selectivity of the LC phases increases along the row: methyl-naphthalenes < xylenes < lutidines < toluidines. Figure 7 shows a typical temperature dependence of the separation factor. The factor depends linearly on reciprocal temperature but more intricately on the generation number. Relationships between the separation factors and the generation number are given in Figure 8. A trend of increasing selectivity of three members G1–G3 is observed for both columnar and isotropic phases. The separation factor decreases upon collapsing the columnar phase and, thus, indicates that the ordering is imposed on the terminal alkyl groups by the columnar molecular packing. However, the selectivity of the dendrimer G4 is drastically lower than that of its lower analogue G3. Such a feature indicates the higher compactness of the terminal group shell of the higher dendrimers.

As a further step, retention indexes of the isomeric solutes (xylenes) and lutidines and corresponding methyl group increments into the indexes have been calculated (Table 4). In all cases the methyl-group increment constitutes ca. 15 % of the index value of the corresponding reference probe (benzene or pyridine). It also tends to increase with the boiling temperature increasing. However, in the case of xylenes, the contribution is a bit higher for the more volatile *para*-isomer. Thus, a factor of structural selectivity inherent in the columnar phase of the dendrimers is manifested. Besides, this factor is manifested as a trend of increasing both index and increment upon increasing the generation number. The trend is clearly observed for all solutes regardless of the molecular geometry.

More features of the dissolution mechanism may be extracted from the temperature dependence of the separation factor. The differences between the enthalpy and entropy contributions into the α value may be calculated from the $\alpha-1/T$ plots (Figure 7) by the

eq 9 (see Background). The contributions are plotted in Figure 9. For all LC phases, the inequality $\Delta(\Delta H_s) \neq T\Delta(\Delta S_s)$ is valid. The location of the correlation plots above the bisector indicates that separation of all probe solutes is determined by the enthalpy factor. Due to increasing the difference between the thermodynamic functions of mixing, the enthalpy factor becomes more and more influential and hence the selectivity increases. The maximal selectivity for all solutes as well as the maximal $\Delta(\Delta H_s)$ and $\Delta(\Delta S_s)$ values are observed for the columnar phase of the dendrimer G3.

Summarizing the data on the retention volumes (Figure 3) and selectivity (Figure 8), one may observe a remarkable feature: the maximal sorption capacity and maximal selectivity are inherent in different dendrimers, namely, G2 and G3, respectively. Thus, the dendrimer G3 exhibits the enhanced selectivity due to high ordering of the terminal groups, whereas its higher free volume is less accessible than the volume of its analog G2. Both other dendrimers G1 and G4 exhibit low capacity and poor selectivity, but these features have seemingly different origins. In the former case, they may be connected with mutual overlapping of the terminal groups of the neighboring macromolecules. In the latter case, a drop in selectivity seemingly results from high compactness of the terminal-group shell.

In conclusion one should note ref 14 where the minimum of the activity coefficient was observed for the amino-terminated dendrimers of intermediate generations. Researchers¹⁴ explained the minimum by an incomplete hydrogenation of the terminal nitrile groups. Our work allows a finer explanation by the effect of shell compactification. If it is the case, one may suppose that the restriction of accessibility of the core by the terminal groups is a general feature of various dendrimers regardless the physical nature of packing interactions. In addition, IGC may be considered as a useful tool for preliminary probing of dendrimers as potential sensors, molecular containers, and so on.

CONCLUSIONS

Sorption behavior of the *n*-hexadecyl-terminated poly(propyleneimine)dendrimers G1–G4 has been studied in the LC and isotropic phases by the inverse gas chromatography technique. Isomeric methyl-substituted derivatives of benzene, pyridine, aniline, and naphthalene were used as probe solutes. A positive deviation from ideality is revealed for all dendrimer–solute systems and rationalized by a governing role of the enthalpy contribution into the Gibbs energy of mixing.

The retention volumes and activity coefficients of the solutes show nonlinear dependences on the generation number. The maximal volumes and minimal coefficients found for the dendrimer G2 indicate the highest thermodynamic compatibility of this dendrimer with the probe solutes. The dendrite sorbents exhibit structural selectivity, the highest selectivity being observed for the dendrimer G3. Thus, structure-imposed sorption restrictions, namely, local ordering and overall compactifying of the terminal-group shell, are revealed. These restrictions exist in both columnar and isotropic phases. They are determined by the generation number and do not depend on the chemical nature of the aromatic solutes.

AUTHOR INFORMATION

Corresponding Author

*E-mail: svb@isc-ras.ru. Phone: 7 (4932)351545. Fax: 7(4932)336246.

REFERENCES

- (1) *Dendrimers and Other Dendritic Polymers*; Frechet, J. M. J., Tomalia, D. A., Eds.; Wiley: Amsterdam, 2001.
- (2) Astruc, D.; Boisselier, E.; Ornelas, C. Dendrimers Designed for Functions: from Physical, Photophysical, and Supramolecular Properties to Applications in Sensing, Catalysis, Molecular Electronics, Photonics, and Nanomedicine. *Chem. Rev.* **2010**, *110*, 1857–1959.
- (3) Newkome, G. R.; Moorefield, C. N.; Vogtle, F. *Dendritic Molecules: Concept, Synthesis, Perspectives*; VCH: Weinheim, 1996.
- (4) Bosman, A. W.; Janssen, H. M.; Meijer, E. W. About Dendrimers: Structure, Physical Properties, and Applications. *Chem. Rev.* **1999**, *99*, 1665–1688.
- (5) Tschierske, C. Non-conventional Liquid Crystals—The Importance of Micro-Segregation for Self-Organisation. *J. Mater. Chem.* **1998**, *8*, 1485–1508.
- (6) Kelker, H. S.; Hatz, R. *Handbook of Liquid Crystals*; Verlag Chemie: Weinheim, 1980.
- (7) Schroeder, J. P. In *Liquid Crystals and Plastic Crystals*; Gray, G. W., Winsor, P. A., Eds.; Holsted Press: New York, 1974; Ch. 7, pp 356–364.
- (8) Witkiewicz, Z.; Oczudłowski, J.; Repelewicz, M. Liquid-Crystalline Stationary Phases for Gas Chromatography. *J. Chromatogr., A* **2005**, *1062*, 155–174.
- (9) Oweimreen, G. A.; Lin, G. C.; Martire, D. E. Thermodynamics of Solutions with Liquid Crystal Solvents. *J. Phys. Chem.* **1979**, *83*, 2111–2119.
- (10) Guillet, J. E.; Al-Saigh, Z. Y. *Inverse Gas Chromatography in the Analysis of Polymers*. In: *Encyclopedia of Analytical Chemistry: Instrumentation and Applications*; Chichester: Wiley, 2000; pp 7759–7792.
- (11) Shillcock, I. M.; Price, G. J. Interactions of Solvents with Low Molar Mass and Side Chain Polymer Liquid Crystals Measured by Inverse Gas Chromatography. *J. Phys. Chem. B* **2004**, *108*, 16405–16414.
- (12) Gritti, F.; Felix, G.; Achard, M. F.; Hardouin, F. Laterally Attached Liquid Crystalline Polymers as Stationary Phases in Reversed-phase High-performance Liquid Chromatography. *J. Chromatogr., A* **2001**, *922*, 51–61.
- (13) Sander, L. C.; Wise, S. A. Effect of Phase Length on Column Selectivity for The Separation of Polycyclic Aromatic Hydrocarbons by Reversed-phase Liquid Chromatography. *Anal. Chem.* **1987**, *59*, 2309–2313.
- (14) Polese, A.; Mio, C.; Bertuccio, A. Infinite-dilution Activity Coefficients of Polar and Nonpolar Solvents in Solutions of Hyperbranched Polymers. *J. Chem. Eng. Data* **1999**, *44*, 839–845.
- (15) Belov, N. A.; Sheremet'eva, N. A.; Yampolskii, Yu. P.; Muzafarov, A. M. Thermodynamics of Sorption of Organic Vapors in Carbosilane Dendrimers and Hyperbranched Polymers. *Polym. Sci. A* **2009**, *51*, 518–530.
- (16) Tande, B. M.; Wagner, N. J.; Kim, Y. H. Influence of End Groups on Dendrimer Rheology and Conformation. *Macromolecules* **2003**, *36*, 4619–4623.
- (17) Vogtle, F.; Richardt, G.; Werner, N. *Functional Dendrimers*. In: *Dendrimer Chemistry Concepts, Syntheses, Properties, Applications*; Wiley: Weinheim 2009; Ch. 3.
- (18) Blokhina, S. V.; Usolt'seva, N. V.; Ol'khovich, M. V.; Sharapova, A. V. Liquid Crystalline Polypropyleneimine Dendrimer as Stationary Phase in Gas Chromatography. *Anal. Chem.* **2007**, *62*, 559–564.
- (19) Blokhina, S. V.; Usolt'seva, N. V.; Ol'khovich, M. V.; Sharapova, A. V. Mesomorphism of Thermotropic Poly(propyleneimine)dendrimers and Phase Equilibria in Systems on Their Basis. *Polym. Sci. A* **2008**, *50*, 322–327.
- (20) Blokhina, S. V.; Usolt'seva, N. V.; Ol'khovich, M. V.; Sharapova, A. V. Thermodynamics of Solution in Liquid Crystalline Poly(propyleneimine) Dendrimers by Inverse Gas Chromatography. *J. Chromatogr., A* **2008**, *1215*, 161–167.
- (21) Blokhina, S. V.; Ol'khovich, M. V.; Sharapova, A. V.; Borovkov, N. Yu. Thermodynamics of Sorption in The Binary Liquid Crystalline System Composed of the Poly(propyleneimine) Dendrimer and *p*-*n*-Pentyloxy-*p'*-cyanobiphenyl by Inverse Gas Chromatography. *J. Phys. Chem. B* **2010**, *114*, 7703–7709.

(22) Mio, C.; Kiritsov, S.; Thio, Y.; Brafman, R.; Prausnitz, J. M. Vapor–liquid Equilibria for Solutions of Dendritic Polymers. *J. Chem. Eng. Data* **1998**, *43*, 541–550.

(23) Lieu, J. G.; Liu, M.; Frechet, J. M. J.; Prausnitz, J. M. Vapor–liquid Equilibria for Dendritic-Polymer Solutions. *J. Chem. Eng. Data* **1999**, *4*, 613–620.

(24) Cameron, J. H.; Facher, A.; Latterman, G.; Diele, S. Poly-(propyleneimine) Dendrosesogens with Hexagonal Columnar Mesophase. *Adv. Mater.* **1997**, *9*, 398–403.

(25) *Handbuch der Gaschromatographie*; Leibnitz, E., Struppe, H. G., Eds.; Geest & Porting: Leipzig, 1984.

(26) Patterson, D.; Tewari, Y. B.; Schreiber, H. P.; Guillet, J. E. Application of Gas-Liquid Chromatography to the Thermodynamics of Polymer Solutions. *Macromolecules* **1971**, *4*, 356–359.

(27) Janini, G. M.; Ubeid, M. T. Thermodynamic of Solutions of Polycyclic Aromatic Hydrocarbons Studied by Gas-Liquid Chromatography with Nematic and Anisotropic Stationary Phase. *J. Chromatogr.* **1982**, *236*, 329–337.

(28) Kovats, E. Gas-Chromatographische Charakterisierung Organischer Verbindungen. Teil 1: Retentionsindices Aliphatischer Halogenide, Alkohole, Aldehyde und Ketone. *Helv. Chim. Acta* **1958**, *41*, 1915–1932.

(29) Reid, R. C.; Prausnitz, J. M.; Sherwood, T. K. *The Properties of Gases and Liquids*; McGraw-Hill Inc.: New York, 1977.